european social fund in the czech republic

EUROPEAN UNION

MINISTRY OF EDUCATION, YOUTH AND SPORTS

OP Education for Competitivness

INVESTMENTS IN EDUCATION DEVELOPMENT

Mapping and modeling species distributions

Department of Botany and Zoology, Masaryk University

Bi9661 Selected issues in Ecology, Autumn 2013

Borja Jiménez-Alfaro, PhD

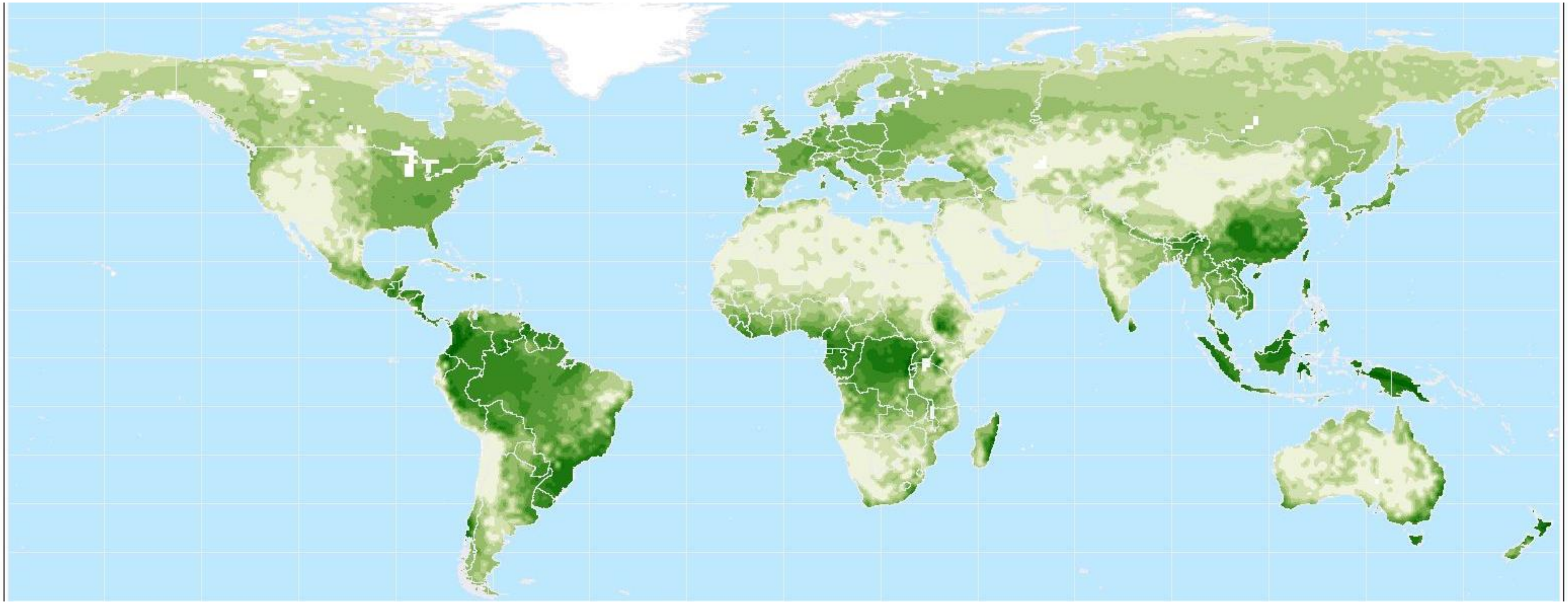

Part 3:

MAPPING + MODELING

Applications

A classification of SDM applications

(adapted from Peterson et al. 2011)

1. The geography of biodiversity
2. Conservation biology
3. Species’ invasions
4. The geography of disease transmision
5. Linking niches with evolutionary processes
6. Other (creative) applications

1. The geography of biodiversity

Possible questions:

What is the distribution of one organism in a given area?

What are the main factors influencing its distribution?

Where can I find similar species?

Guisan et al. 2006

Improvement of sampling design and distribution of rare species

Conservation Biology Volume 20, No. 2, 501–511
©2006 Society for Conservation Biology
DOI: 10.1111/j.1523-1739.2006.00354.x

Using Niche-Based Models to Improve the Sampling of Rare Species

ANTOINE GUISAN,*†† OLIVIER BROENNIMANN,* ROBIN ENGLER,* MATHIAS VUST,*
NIGEL G. YOCCOZ,† ANTHONY LEHMANN,§ AND NIKLAUS E. ZIMMERMANN‡

*University of Lausanne, Department of Ecology and Evolution (DEE), Laboratory for Conservation Biology (LBC), Biology Building, CH-1015 Lausanne, Switzerland
†Institute of Biology, University of Tromsø, 9037 Tromsø, Norway
‡Swiss Federal Research Institute WSL, Zürcherstrasse 111, CH-8903 Birmensdorf, Switzerland
§Swiss Center for Faunal Cartography, Terreaux 14, CH-2000 Neuchâtel, Switzerland

Guisan et al. 2006

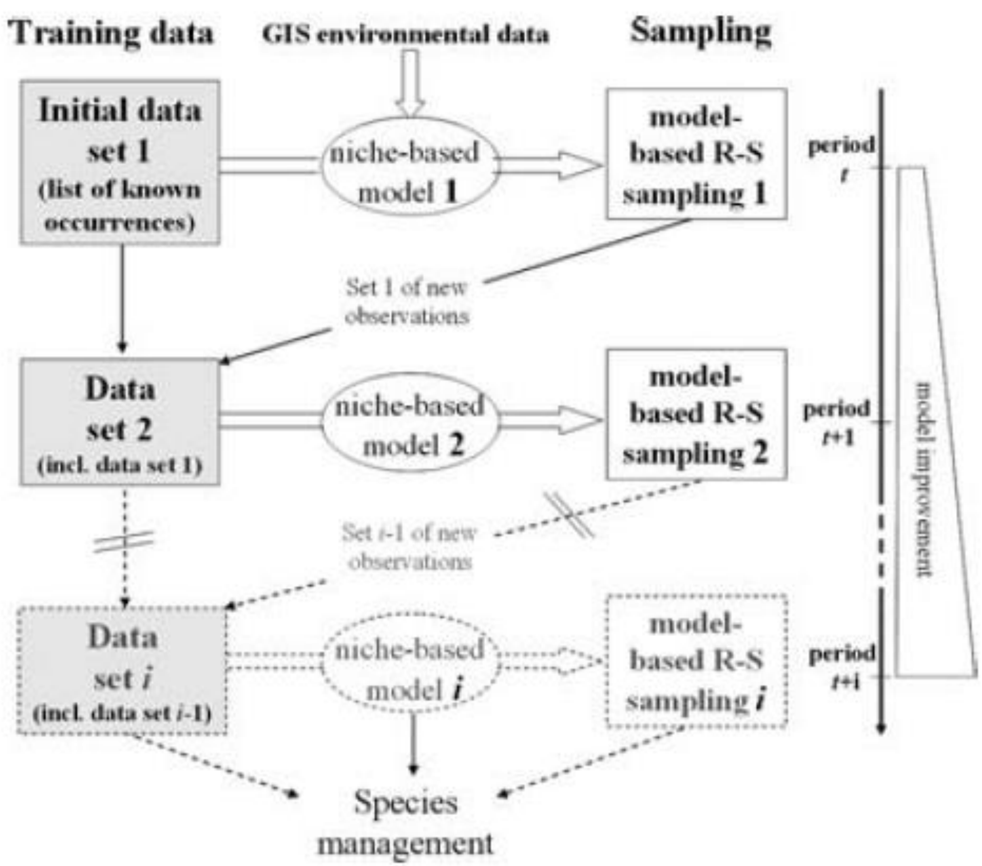

Figure 1. Analytical procedure illustrating the iterative model-based sampling process.

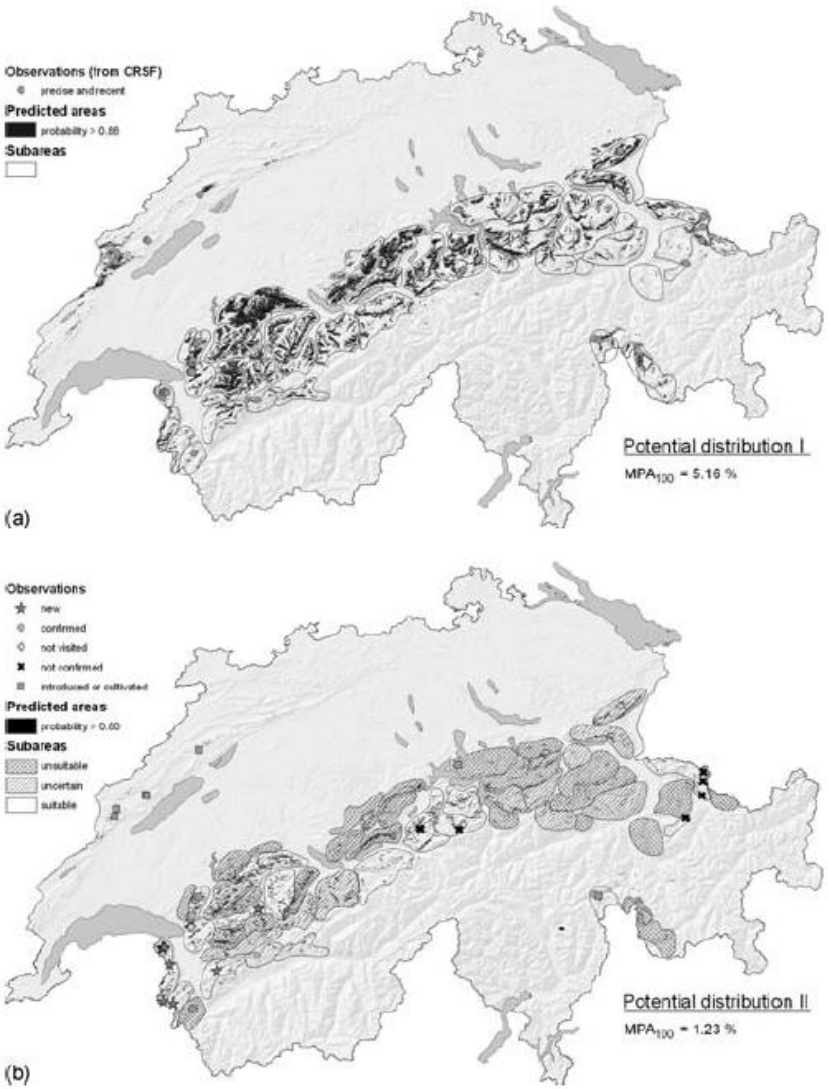

Figure 2. Potential distribution maps for Eryngium alpinum *in Switzerland. (a) Model 1, used to stratify the sampling. Subareas used for sampling are also shown (polygons; see text). Observations correspond to recent (1995 or later) and precise (25-m accuracy) observations. (b) Model 2, improved from model 1 with data sampled in the field. Updated knowledge on geological units important for the species, derived from the field campaign, is also shown (polygons with various shading). The predicted area appears in both maps as dark grey and corresponds to the minimal predicted area (MPA; see methods) containing 100% of observations (MPA_{100}).*

Miller & Franklin 2002

Distribution models for plant communities (alliances)

ELSEVIER

Ecological Modelling 157 (2002) 227–247

ECOLOGICAL MODELLING

www.elsevier.com/locate/ecolmodel

Modeling the distribution of four vegetation alliances using generalized linear models and classification trees with spatial dependence☆

Jennifer Miller *, Janet Franklin

Department of Geography, San Diego State University, San Diego, CA 92182-4493, USA

Received 15 June 2001; received in revised form 25 February 2002; accepted 16 April 2002

Miller & Franklin 2002

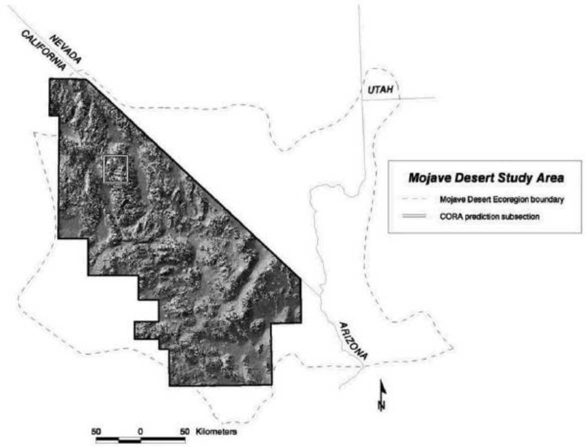

Fig. 1. The Mojave Desert Study Area (box shows mapped subsection for CORA predictions used in Figs. 5 and 6).

Table 2
Vegetation alliances modeled

Label	Alliance name	*n* test	*n* train	Dominant and indicator species	Habitat
ATCA	*Atriplex canascens* — Shrubland alliance	7	16	*A. canascens*, *Bromus madritensis*	Margins of playas
CORA	*Coleogyne ramosissima* — Shrubland alliance	21	110	*C. ramosissima*, *Atriplex confertifolia*, *Ephedra nevadensis*, *Ephedra viridis*, *Eriogonum fasciculatum*, *Salizaria mexicana*	Widespread: shallow rocky soils on upper bajadas, pediments and hill slopes
PIMO	*Pinus monophylla* — Woodland alliance	12	38	*P. monophylla*, *Artemisia tridentata*, *Quercus cornelius-mulleri*, *Nama californica*	Upper elevations: cool, moist mountain areas
YUBR	*Yucca brevifolia* — Wooded shrubland alliance	87	265	*Y. brevifolia*, *Artemisia tridentata*, *Artemisia confertifolia*, *C. ramosissima*, *Opuntia acanthocarpa*	Narrow zone, base of mountains

The data set of 3819 observations was divided randomly into a 75% train and 25% test subsets. *n* test gives the number of observations present in the $n = 960$ test dataset; *n* train gives the number of observations present in the $n = 2859$ training dataset.

Miller & Franklin 2002

Table 1
Environmental variables used in this study

Variable name	Variable
Sumprecip	Average summer precipitation
Winprecip	Average winter precipitation
Jantemp	Minimum January temperature
Jultemp	Maximum July temperature
Elevation	Elevation; from USGS 7.5' DEM
Slope	Slope
Swness	Cosine(aspect − 225°) (Franklin et al., 2000)
Lpos4	Landscape position; Average difference between cell and neighbors; positive in valleys, neutral in mid-slope position, and negative on ridges (Fels, 1994)
Solrad	Solar radiation (Dubayah, 1994)
TMI	Topographic moisture index; number of cells draining into a cell divided by the tangent of slope (Beven and Kirkby, 1979)
Landform	Geomorphic landform (Dokka et al., 1999)
Landcomp	Surface composition

Climate variables are 1 km resolution; all others are 30 m resolution.

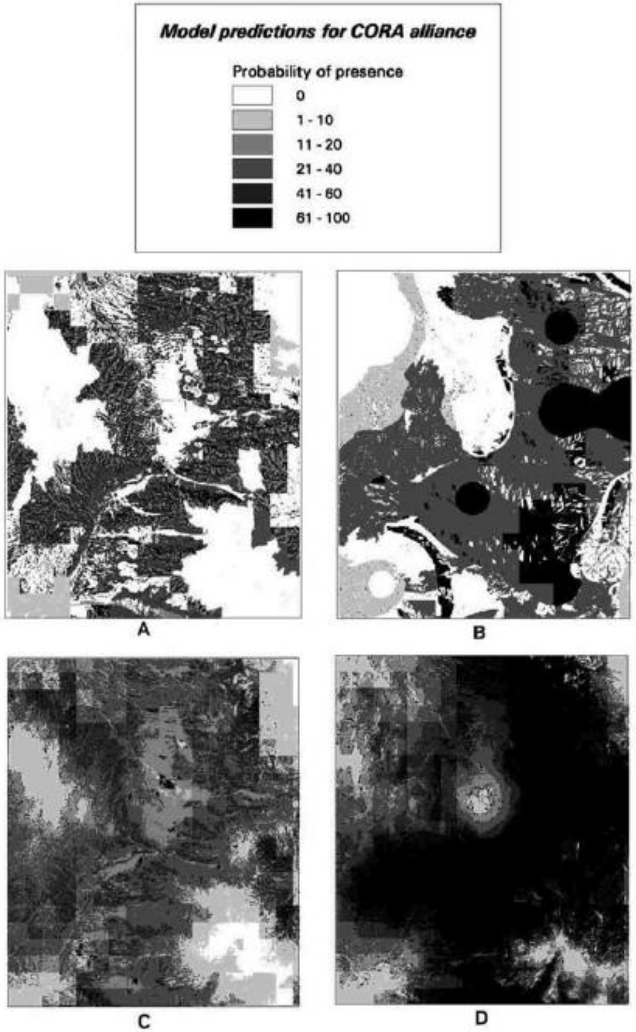

Fig. 6. Predictions generated for test area with (A) CORA classification tree ($P=0.1$); (B) CORA classification tree with kriged dependence term ($P=0.2$); (C) CORA GLM ($P=0.2$); (D) Cora GLM with kriged dependence term ($P=0.2$). Optimum probability thresholds are given in parentheses.

2. Conservation biology

Possible questions:

What are the main conservation areas for a species?

How rare is one species in one area?

What will be the effect of climate change on species distributions?

Thorn et al, 2009

They apply Maxent to assess conservation priorities

Diversity and Distributions, (Diversity Distrib.) (2009) 15, 289–298

BIODIVERSITY RESEARCH

Ecological niche modelling as a technique for assessing threats and setting conservation priorities for Asian slow lorises (Primates: *Nycticebus*)

J. S. Thorn*, V. Nijman, D. Smith and K. A. I. Nekaris

Thorn et al, 2009

Table 1 Criteria for qualifying habitat patches as low, medium or high risk. The ranking indicates the suitability of habitat patches for supporting viable populations of *Nycticebus*.

Measure	Low risk	Medium risk	High risk
Size of forest patch	> 40 km^2	> 20 km^2	> 10 km^2
Proximity to protected areas	Within 20 km*	Within 20–30 km	Within 30–40 km
Proximity to populated areas	> 10 km	> 5 km	Adjacent
Proximity to roads	> 10 km	> 5 km	Adjacent
Proximity to agriculture	> 5 km	> 2.5 km	Adjacent

*For *N. menagensis* 'Proximity to protected area', the low risk criterion was within 20 km of protected area network or inside the Heart of Borneo.

Table 2 Results of the jackknife validation method of model testing for *Nycticebus coucang*, *N. javanicus* and *N. menagensis*, showing the sample sizes included for modelling, and the data used to calculate the *P*-values.

Species	Locality sample size	Number of successes	Mean fractional predicted area	Lowest presence threshold (LPT)	*P*-value
N. coucang	15	13	0.54	18.664	0.006
N. javanicus	10	9	0.49	12.523	0.003
N. menagensis	23	21	0.72	4.886	0.027

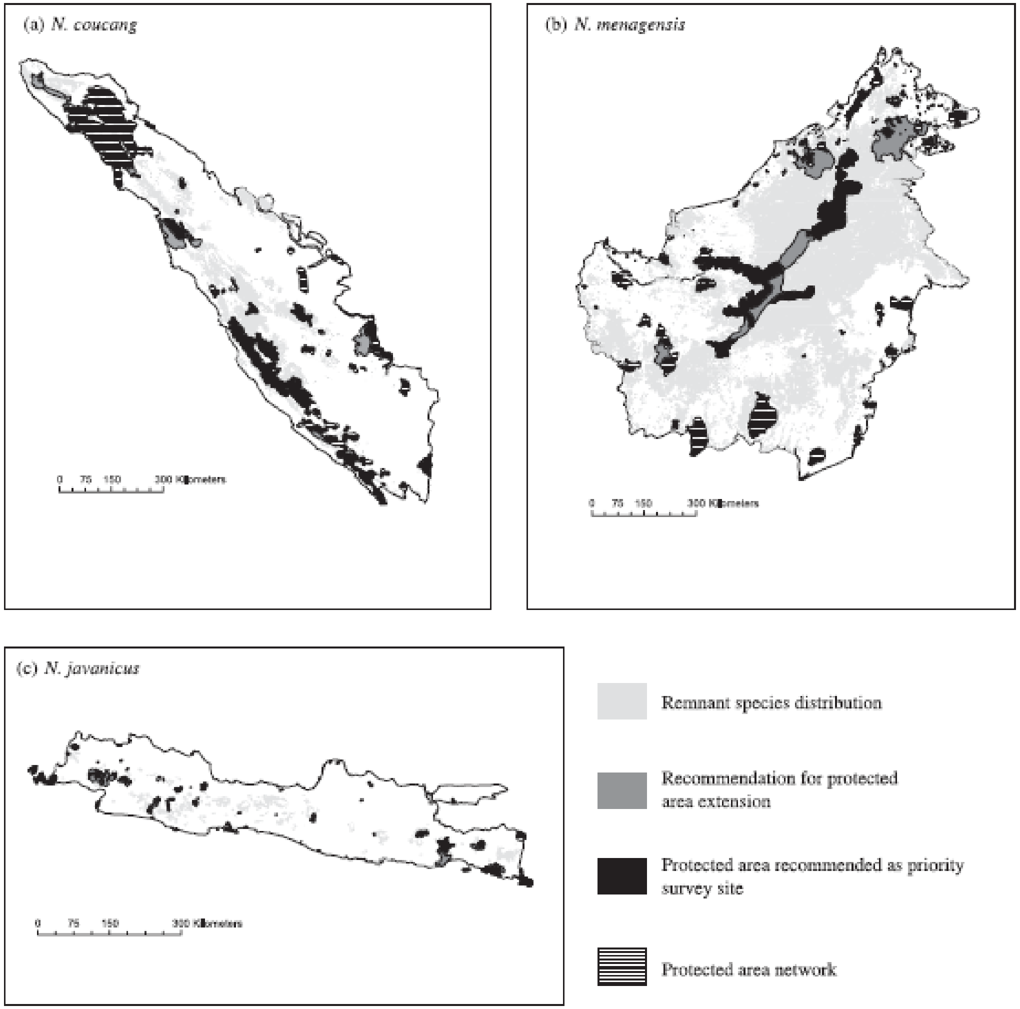

Figure 3 Recommendations for protected area extensions and priority survey areas based on species remnant distributions and results of the risk assessment for (a) *Nycricebus coucang* on Sumatra, (b) *N. menagensis* on Borneo, and (c) *N. javanicus* on Java. Protected area extensions are shown in dark grey and priority survey areas are shown in black.

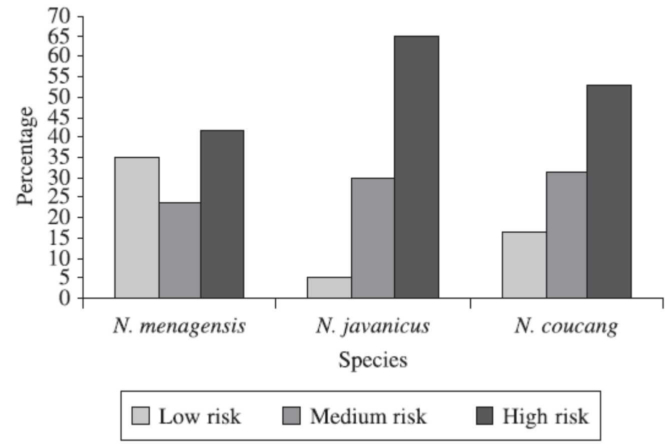

Figure 2 Percentage of suitable habitat classified as low risk, medium risk or high risk for *Nycticebus menagensis*, *N. javanicus* and *N. coucang* according to the risk assessment criteria.

Jiménez-Alfaro et al. 2012

Estimation of the AOO to estimate local distribution ranges

ELSEVIER

Contents lists available at SciVerse ScienceDirect

Biological Conservation

journal homepage: www.elsevier.com/locate/biocon

Modeling the potential area of occupancy at fine resolution may reduce uncertainty in species range estimates

Borja Jiménez-Alfaro [a,*], David Draper [b], David Nogués-Bravo [c]

[a] Jardín Botánico Atlántico, University of Oviedo, Av. del Jardín Botánico 2230, 33394 Gijón, Spain
[b] Dep. Biología Vegetal, ETSI, Universidad Politécnica de Madrid, Av. Complutense s/n. Ciudad Universitaria, 28040 Madrid, Spain
[c] Center for Macroecology, Evolution and Climate, University of Copenhagen, Denmark

Jiménez-Alfaro et al. 2012

Table 1
Explanatory variables used to fit species distribution models for *Empetrum nigrum* and absolute ranges for the study area. All variables were derived from a Digital Elevation Model (DEM) at 15 m × 15 m resolution, and included as continuous environmental variables in MaxEnt software (Phillips et al., 2006).

Variable	Min–Max	Description
Altitude	1570–2150	Elevation (m) derived from DEM
Slope	0–75	Slope degrees generated from DEM
Radiation	1496–7466	Annual global solar radiation (WM^2) derived from altitude, exposure and solar trajectory
Curvature	−73 to 86	Indirect variable related to flow accumulation, reflecting concavity (<0) or convexity (>0)
Aspect (Northness)	−1 to 1	Cos (aspect)*sen (slope)
Aspect (Easterness)	−1 to 1	Sen (aspect)*sen (slope)

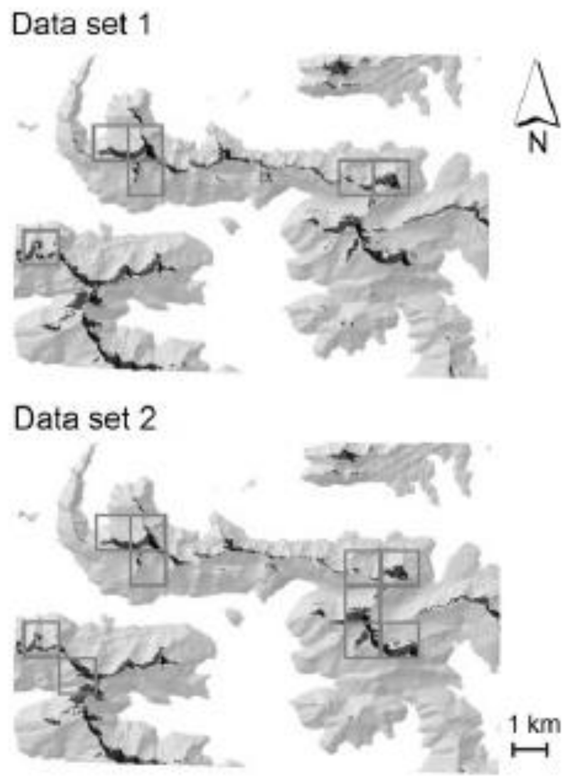

Fig. 1. Potential area of occupancy estimated for *Empetrum nigrum* along its known distribution area in Spain, using two data sets obtained from expert (Data set 1) and systematic (Data set 2) surveys. Dark colors show model-based estimates using maximum entropy algorithm and the minimal predicted area as probability threshold. Grid (gray) cells represent the AOO that would be measured using the occurrence of the species in 1 km × 1 km grids.

Jiménez-Alfaro et al. 2012

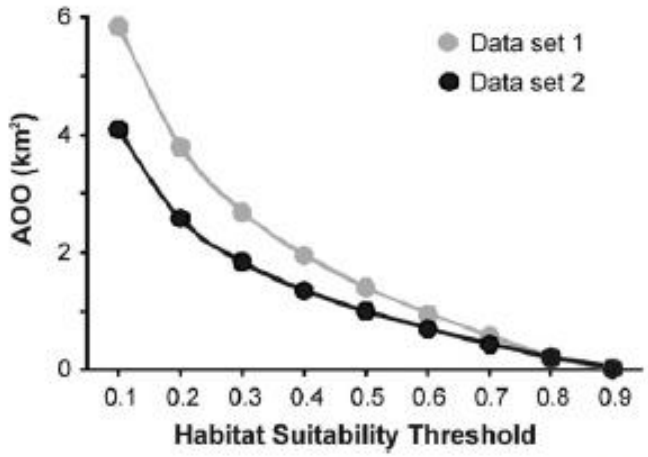

Fig. 2. Sensitivity of species distribution models to different thresholds of habitat suitability, according to the total Area of Occupancy (AOO) measured when using presence data obtained from expert (Data set 1) and systematic (Data set 2) surveys.

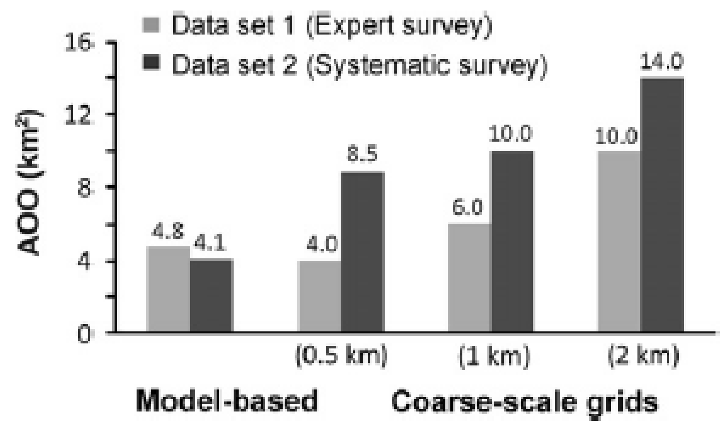

Fig. 3. Total estimates of Area of Occupancy (AOO) for *Empetrum nigrum* in Spain, according to different survey protocols (Data set 1 and 2) and alternative measurements of model-based methods (based on fine-resolution models and the minimal predicted area) and coarse-scale grids (based on reported localities) at different accuracy.

3. Species' invasions

Possible questions:

What is the niche of invasive species?

What is the risk of species' invasion in one region?

How invasive species adapt to climatic changes?

Broennimann et al. 2007

Comparing the niche of an invasive plant in two continents

Ecology Letters, (2007) **10:** 701–709 doi: 10.1111/j.1461-0248.2007.01060.x

LETTER

Evidence of climatic niche shift during biological invasion

O. Broennimann,[1] U. A. Treier,[2,3] H. Müller-Schärer,[2] W. Thuiller,[4] A. T. Peterson[5] and A. Guisan[1]

Abstract

Niche-based models calibrated in the native range by relating species observations to climatic variables are commonly used to predict the potential spatial extent of species' invasion. This climate matching approach relies on the assumption that invasive species

Broennimann et al. 2007

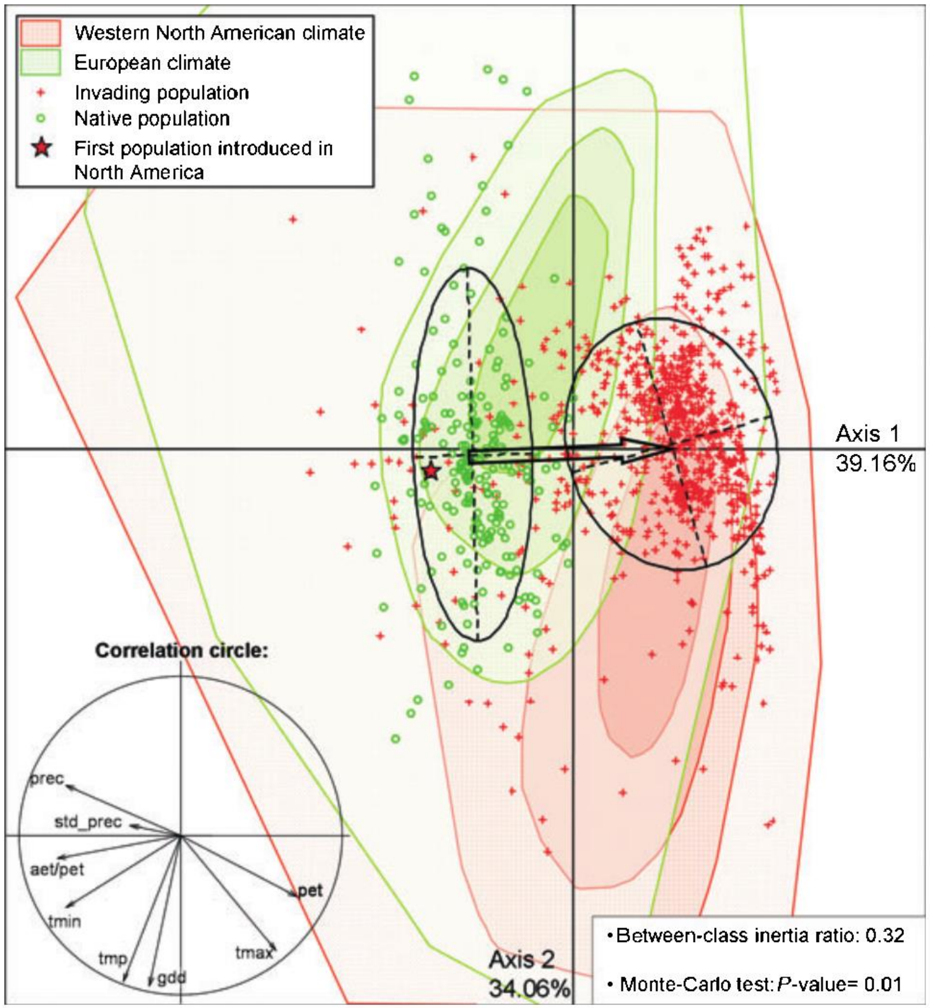

Table 1 List of predictors available in each climatic data set

Data set	Variable	Description
WORLDCLIM	BIO1	Annual mean temperature
	BIO2	Mean diurnal range
	BIO3	Isothermality
	BIO4	Temperature seasonality
	BIO5	Max temperature of warmest month
	BIO6	Min temperature of coldest month
	BIO7	Temperature annual range
	BIO8	Mean temperature of wettest quarter
	BIO9	Mean temperature of driest quarter
	BIO10	Mean temperature of warmest quarter
	BIO11	Mean temperature of coldest quarter
	BIO12	Annual precipitation
	BIO13	Precipitation of wettest month
	BIO14	Precipitation of driest month
	BIO15	Precipitation seasonality
	BIO16	Precipitation of wettest quarter
	BIO17	Precipitation of driest quarter
	BIO18	Precipitation of warmest quarter
	BIO19	Precipitation of coldest quarter
CRU 10′	aet/pet	Ratio of actual to potential evapotranspiration
	pet	Potential evapotranspiration
	prec	Annual amount of precipitations
	std_prec	Annual variation of precipitations
	tmin	Minimum temperature of the coldest month
	tmp	Annual mean temperature
	tmax	Maximum temperature of the warmest month
	gdd	Growing degree-days above 5 °C
CRU 0.5°	tmin	Minimum temperature of the coldest month
	tmp	Annual mean temperature
	tmax	Maximum temperature of the warmest month
	rad	Annual amount of radiations
	prec	Annual amount of precipitations

Broennimann et al. 2007

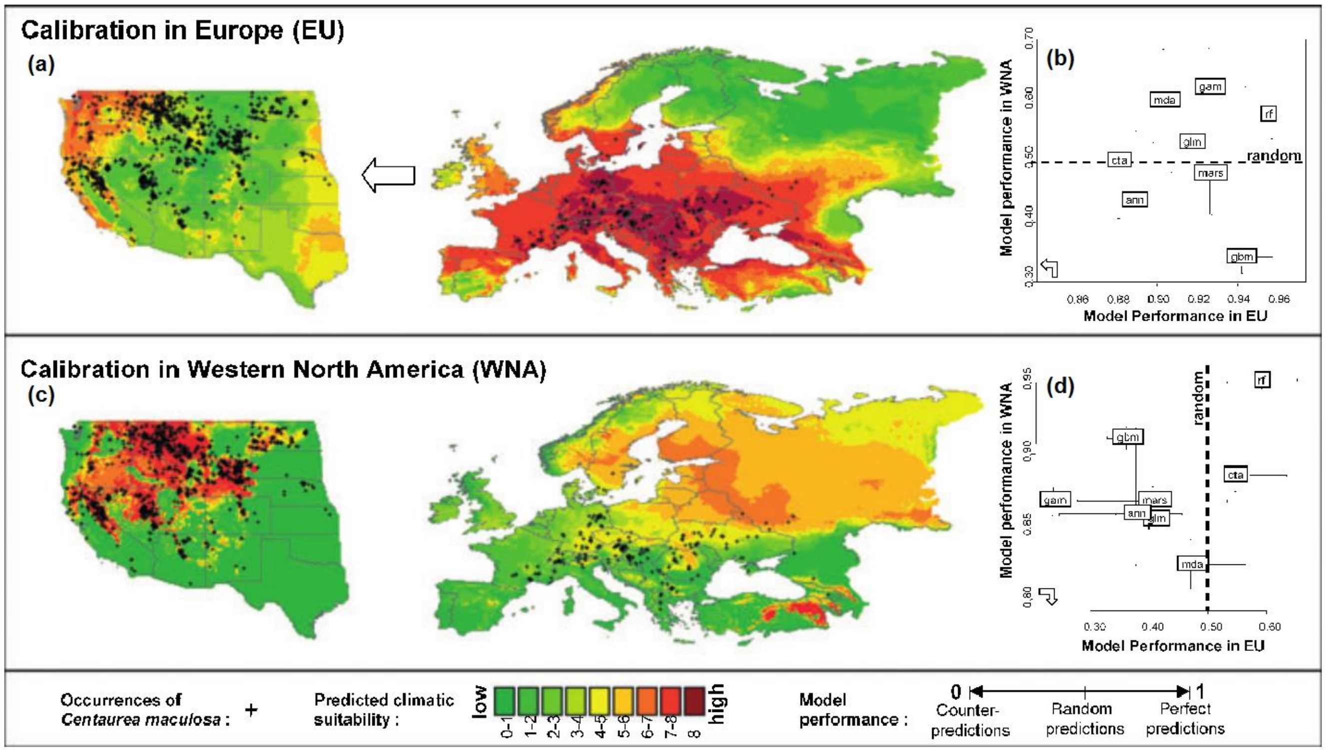

Figure 2 Prediction maps and model evaluation. The upper and lower boxes illustrate, respectively, the results obtained from models calibrated in Europe (EU; a, b) and Western North America (WNA; c, d), and projected into the other range. The maps (a, c) show the predicted climatic suitability (mean number of models, among eight modelling techniques, predicting the species present). The series of graphs (b, d) plot model performance [area under the curve (AUC)] for 100 repetitions of each technique, based on random re-sampling of the data. The AUC (see Supplementary Material) of a receiver-operating characteristic (ROC) curve calculated on independent data is currently the most objective measure of model performance for presence–absence data, with 1 indicating perfect prediction, 0.5 not different than random and 0 a perfect counter prediction. The horizontal axis indicates the model performance of the predictions in the native area (EU). The vertical axis indicates the model performance of the predictions in the invaded area (WNA). The horizontal and vertical dashed lines indicate predictions that do not differ from random (AUC ¼ 0.5) when projected in the other area (WNA in b; EU in d). Error bars indicate the standard deviation

Benedict et al. 2007

Ecological risk map for the most invasive mosquito in the world

Published in final edited form as:
Vector Borne Zoonotic Dis. 2007 ; 7(1): 76–85.

Spread of the Tiger: Global Risk of Invasion by the Mosquito *Aedes albopictus*

MARK Q. BENEDICT[1], **REBECCA S. LEVINE**[1], **WILLIAM A. HAWLEY**[1], and **L. PHILIP LOUNIBOS**[2]

1 *Centers for Disease Control and Prevention, Atlanta, Georgia*

2 *University of Florida, Florida Medical Entomology Laboratory, Vero Beach, Florida*

Benedict et al. 2007

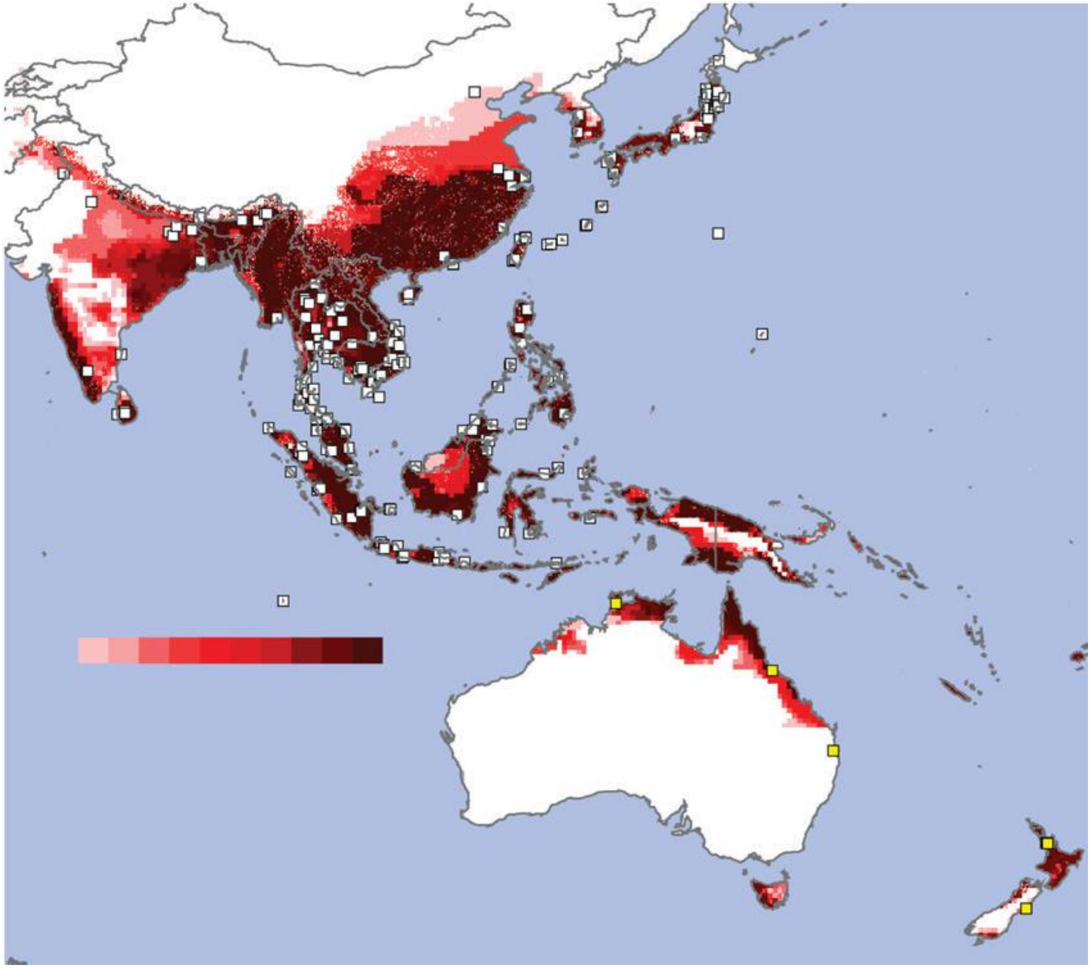

FIG. 1.
Predicted Australasian range map of *Ae. albopictus*. Darker shades indicate pixels for which higher numbers of models predicted potential suitable niches with the darkest shades signifying 10 models. The legend bar shows the 10 colors used. White squares represent the known occurrence points used to create the models. Yellow squares are known introduction sites outside of the native range.

Benedict et al. 2007

Table 2

Annual Values for Climatic Environmental Variables at 408 Random Geo-Referenced Points where *Ae. albopictus* Occurs Worldwide

Environmental characteristic	Range	Mean	Median
Mean annual temperature (°C)	5.0–28.5	21.5	23.4
Mean maximum annual temperature (°C)	8.2–33.4	26.3	28.55
Mean annual minimum temperature (°C)	−1.8–24.4	16.7	18.3
Mean annual precipitation (cm)	29.2–445.3	169.0	157.0
Mean annual wet days (*n*)	30.0–280.8	167.6	169.2
Ground-frost days/month (*n*)	0–138	14.9	0

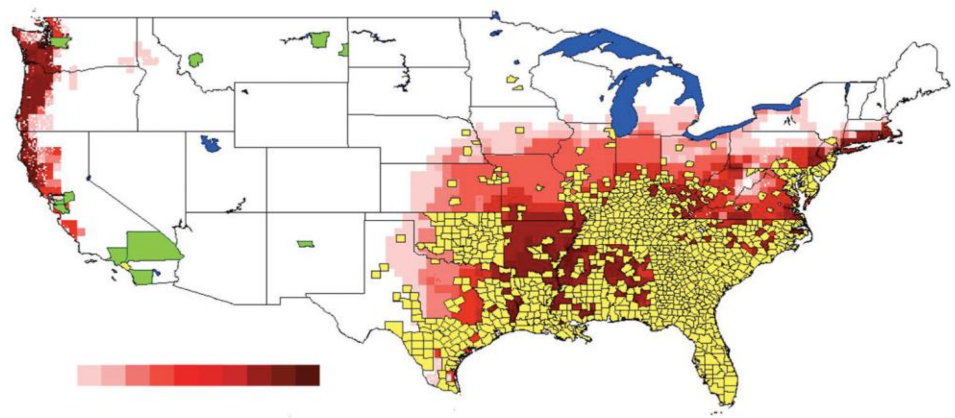

DesktopGarp

FIG. 3.
Predicted distribution maps and actual spread of *Ae. albopictus* in the lower 48 states. The predicted distribution areas (red) and the documented spread (yellow) of *Ae. albopictus* through the year 2001 are shown. One of the two prediction maps for the US is shown. Differences between the two consisted largely of one of the ten models used to create the prediction map that predicted a broader Texas distribution. Counties colored green are those in which introduction has occurred but not establishment.

4. The geography of desease transmision

Possible questions:

What is the distribution area of a desease?

What are the main factors related to vectors and hosts?

What areas can be potentially affected by a desease?

Peterson 2009

Potential distribution of malaria vectors under climate warming

BMC Infectious Diseases

BioMed Central

Research article

Open Access

Shifting suitability for malaria vectors across Africa with warming climates

A Townsend Peterson

Address: Biodiversity Research Center, The University of Kansas, Lawrence, Kansas 66045, USA

Email: A Townsend Peterson - town@ku.edu

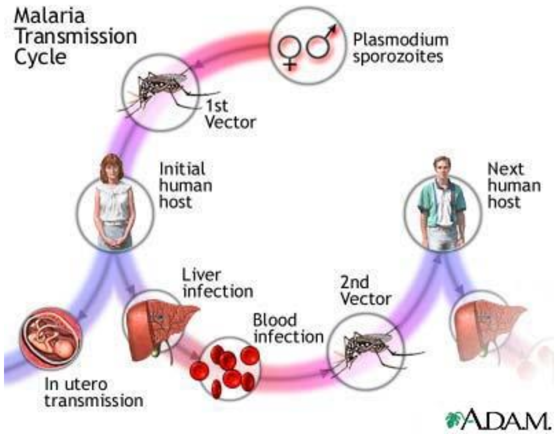

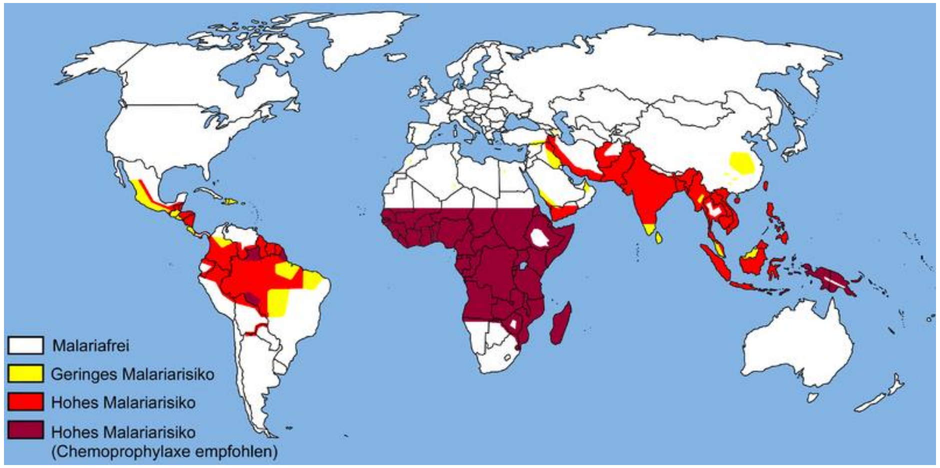

Peterson 2009

Human population *Anopheles gambiae* *Anopheles arabiensis*

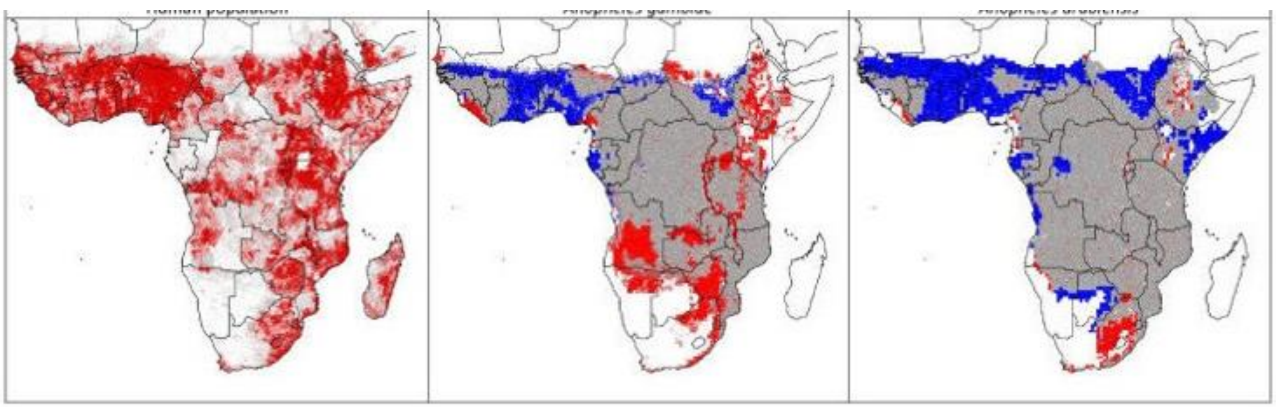

GARP

Suitable both in present and in the future

Presently suitable, not in the future

Newly suitable in the future

Hay et al. 2013

Mapping infectious desease occurrence requires new models

PHILOSOPHICAL TRANSACTIONS OF THE ROYAL SOCIETY B

rstb.royalsocietypublishing.org

Review

CrossMark

Global mapping of infectious disease

Simon I. Hay[1,2], Katherine E. Battle[1], David M. Pigott[1], David L. Smith[2,3], Catherine L. Moyes[1], Samir Bhatt[1], John S. Brownstein[4], Nigel Collier[5], Monica F. Myers[1], Dylan B. George[2] and Peter W. Gething[1]

[1]Spatial Ecology and Epidemiology Group, Department of Zoology, University of Oxford, Oxford, UK
[2]Fogarty International Center, National Institutes of Health, Bethesda, MD, USA
[3]Department of Epidemiology and Malaria Research Institute, Johns Hopkins Bloomberg School of Public Health, Baltimore, MD, USA
[4]Department of Pediatrics, Harvard Medical School and Children's Hospital Informatics Program, Boston Children's Hospital, Boston, MA, USA
[5]National Institute of Informatics, Research Organization of Information and Systems, Tokyo, Japan

Hay et al. 2013 Conceptual scheme (with boosted regression trees)

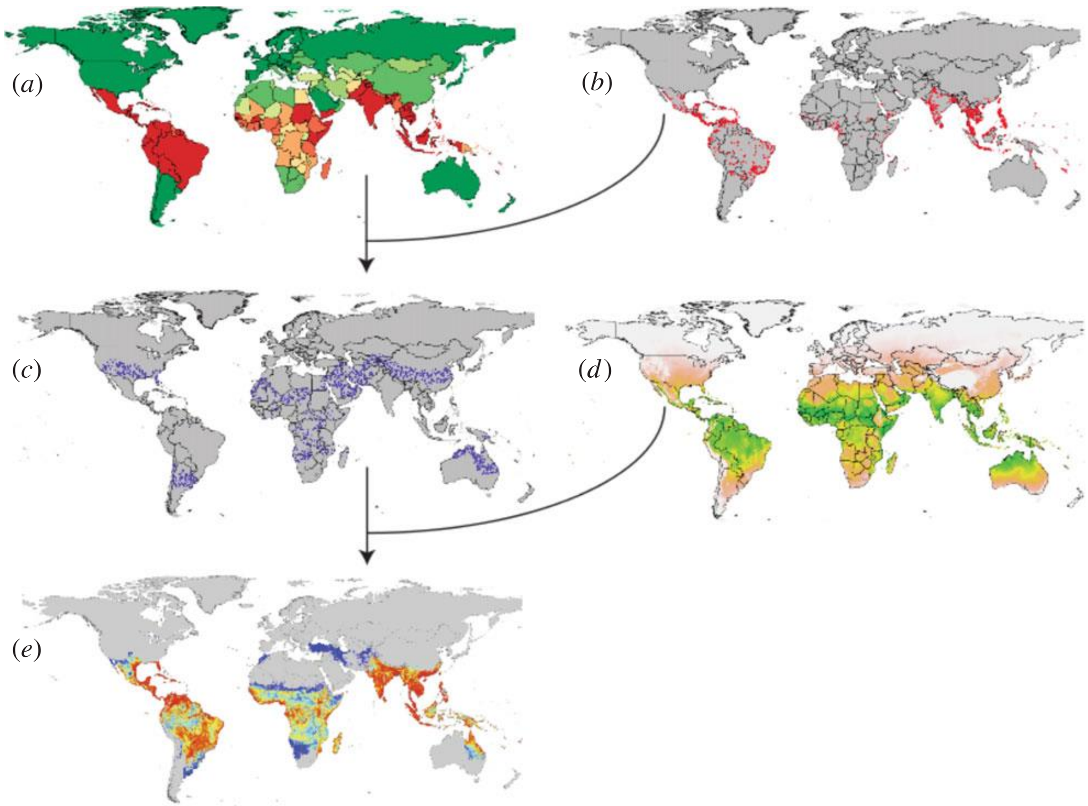

Figure 1. A schematic overview of a niche/occurrence mapping process (for example boosted regression trees (BRT)) that uses pseudo-absence data guided by expert opinion. Consensus based definitive extent layers of infectious disease occurrence at the national level (*a*) are combined with accurately geo-positioned occurrence (presence) locations (*b*) to generate pseudo-absence data (*c*). The presence (*b*) and pseudo-absence data (*c*) are then used in the BRT analyses, alongside a suite of environmental covariates (*d*) to predict the probability of occurrence of the target disease (*e*).

5. Linking niches with evolutionary processes

Possible questions:

How species niches relate to phylogeography?

How the ecological niche of species change along the time?

Are species subjected to niche conservatism?

Jakob et al. 2007

Differentiation processes: genetic vs. ecological variation

Molecular Ecology (2007) doi: 10.1111/j.1365-294X.2007.03228.x

Combined ecological niche modelling and molecular phylogeography revealed the evolutionary history of *Hordeum marinum* (Poaceae) — niche differentiation, loss of genetic diversity, and speciation in Mediterranean Quaternary refugia

SABINE S. JAKOB, ALEXANDER IHLOW and FRANK R. BLATTNER
Leibniz Institute of Plant Genetics and Crop Sciences (IPK), Corrensstr. 3, D-06466 Gatersleben, Germany

Jakob et al. 2007

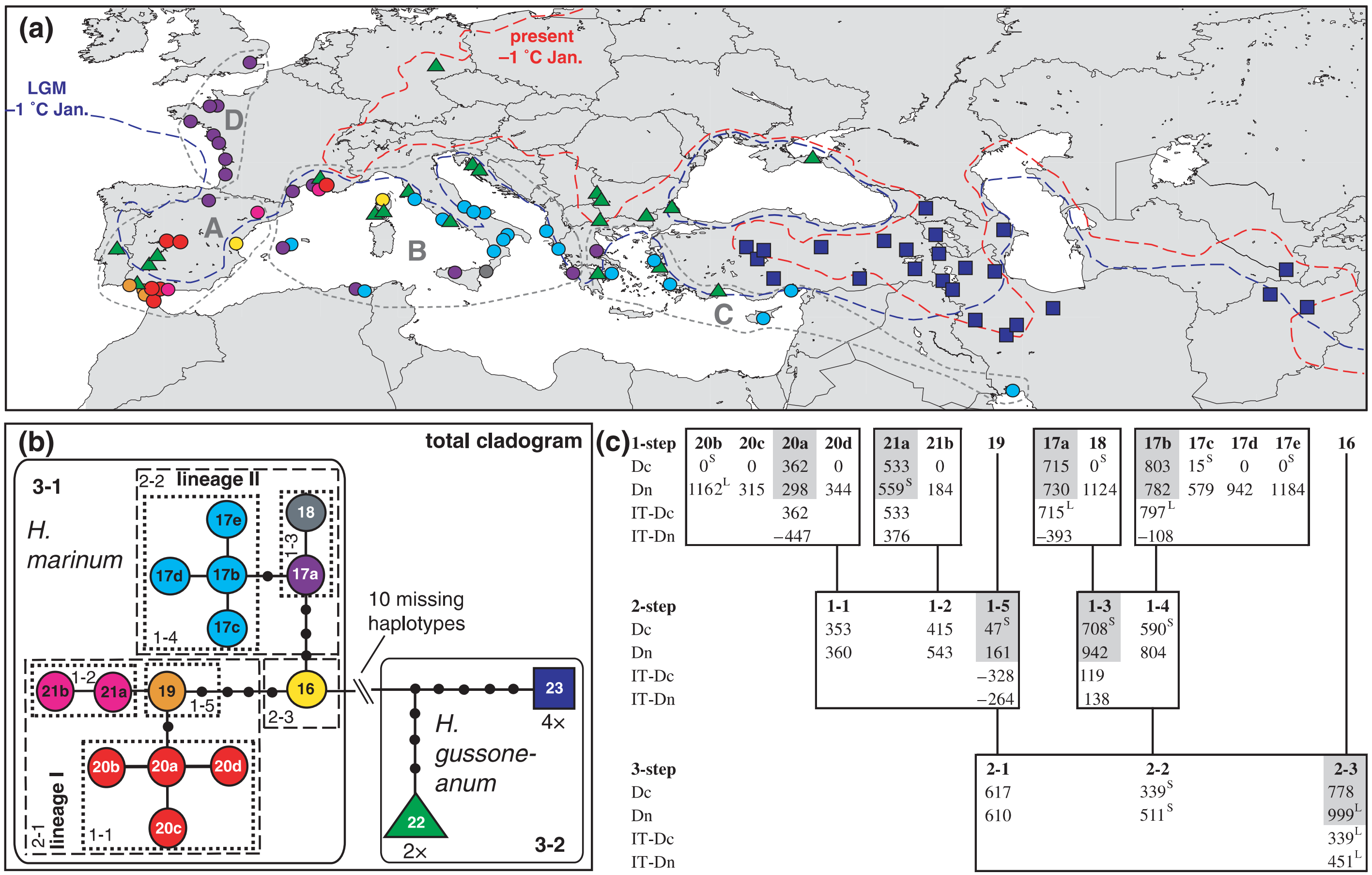

Fig. 1 (a) Geographical distribution of *Hordeum marinum s.l.* chloroplast haplotypes. Circles indicate *H. marinum*, triangles *Hordeum gussoneanum* 2×, and squares *H. gussoneanum* 4×. The colours of the symbols refer to Fig. 1 (b). Regional subdivision into four geographical areas (a–d) is indicated (see Table 4). The dashed lines indicate the approximate position of the –1°C January isotherm, in blue during the last glacial maximum (LGM) about 20 000 years ago, in red at present (based on data of the STAGE THREE project, http://

Jakob et al. 2007

BIOCLIM
In DIVA-GIS

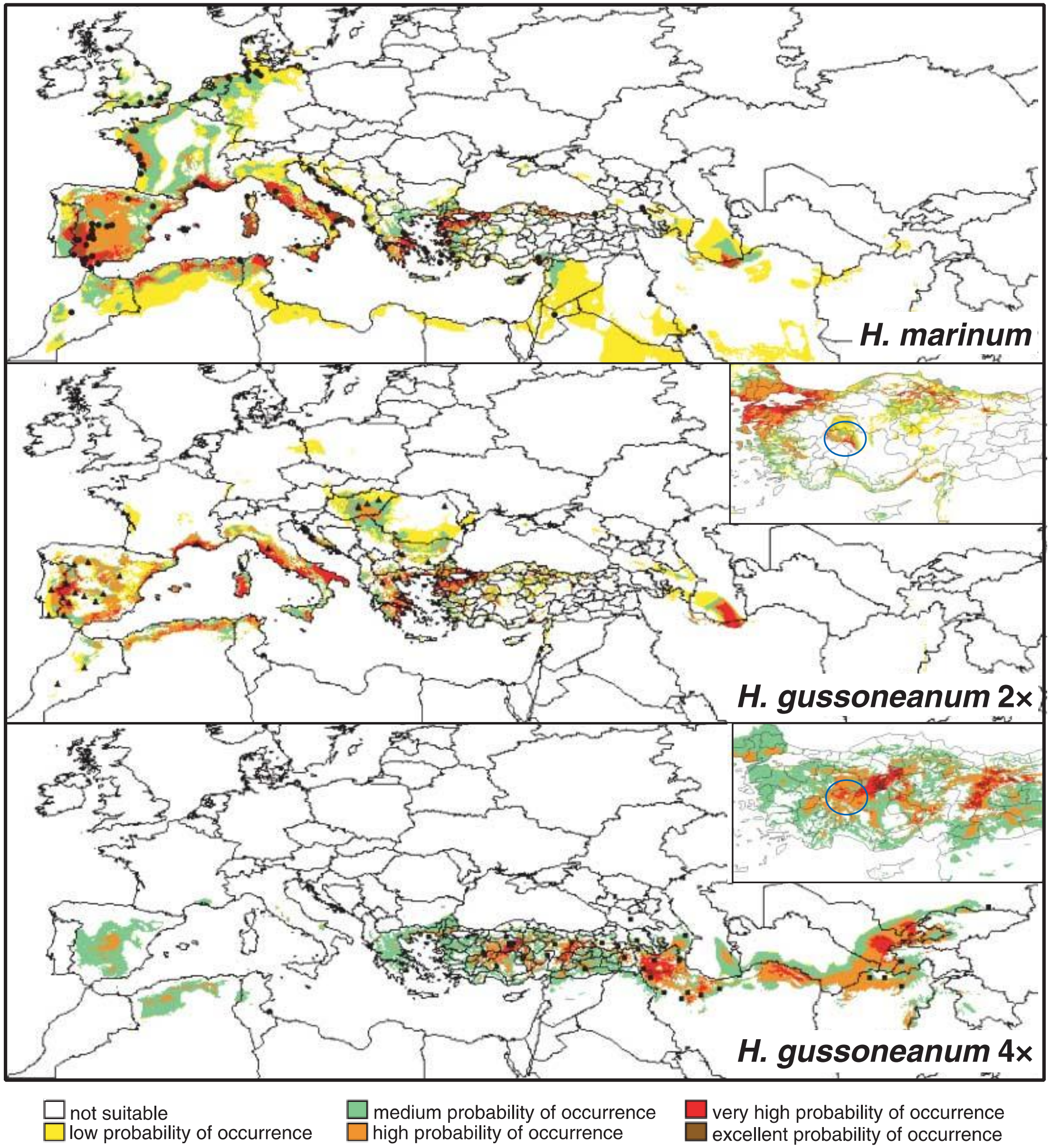

Martínez-Meyer & Peterson 2006

Testing niche conservatism in eight species with pollen records

Journal of Biogeography (*J. Biogeogr.*) (2006) **33**, 1779–1789

SPECIAL ISSUE

Conservatism of ecological niche characteristics in North American plant species over the Pleistocene-to-Recent transition

E. Martínez-Meyer[1*] and A. T. Peterson[2]

Martínez-Meyer & Peterson 2006

Table 1 Summary of reciprocal tests of predictivity of geographic distributions based on ecological niche characteristics for pollen records of eight plant species, predicting from Last Glacial Maximum ('Pleistocene') to present, and vice versa. Ten best-subsets models were developed for each reciprocal prediction for each species; 'all' refers to 10 of 10 models predicting presence, 'most' refers to >5 of 10 models predicting presence, and 'any' refers to at least 1 of 10 models predicting presence

	Proportional area predicted present				Number of test points successfully predicted			Binomial probability		
Species	All	Most	Any	*n*	All	Most	Any	All	Most	Any
Pleistocene predicts present										
Acer rubrum	0.178	0.272	0.438	103	58	75	88	2.33×10^{-15}	0	-8.4×10^{-15}
Acer saccharum type	0.170	0.394	0.772	131	82	116	130	2.89×10^{-15}	0	-2×10^{-15}
Alnus incana	0.247	0.457	0.720	101	49	63	92	6.79×10^{-8}	0.000261	5.28×10^{-7}
Alnus viridis	0.258	0.376	0.600	109	55	70	87	1.04×10^{-8}	5.11×10^{-9}	3.06×10^{-6}
Brasenia schreberi	0.102	0.285	0.568	30	13	25	29	3.88×10^{-7}	5.09×10^{-11}	4.27×10^{-8}
Fraxinus nigra type	0.391	0.629	0.886	112	80	104	111	1.14×10^{-12}	3.2×10^{-14}	1.25×10^{-6}
Juglans cinerea	0.310	0.570	0.835	77	36	60	74	0.001284	3.54×10^{-5}	0.000124
Sarcobatus vermiculatus	0.093	0.299	0.702	94	34	66	88	2.19×10^{-13}	2.78×10^{-15}	3.01×10^{-9}
Present predicts Pleistocene										
Acer rubrum	0.115	0.163	0.236	6	5	5	5	2.32×10^{-6}	1.89×10^{-5}	0.000171
Acer saccharum type	0.079	0.142	0.235	6	2	4	4	0.008149	0.000305	0.00345
Alnus incana	0.029	0.149	0.277	7	0	2	5	0.184569	0.072542	0.002392
Alnus viridis	0.015	0.130	0.310	7	0	2	3	0.100394	0.050975	0.138968
Brasenia schreberi	0.070	0.140	0.230	6	2	4	6	0.005867	0.000289	$<10^{-10}$
Fraxinus nigra type	0.072	0.153	0.272	7	2	4	6	0.01038	0.001329	0.000109
Juglans cinerea	0.071	0.131	0.243	6	3	3	4	0.000337	0.003593	0.004081
Sarcobatus vermiculatus	0.145	0.219	0.282	5	3	4	4	0.001968	0.000501	0.001771

Martínez-Meyer & Peterson 2006

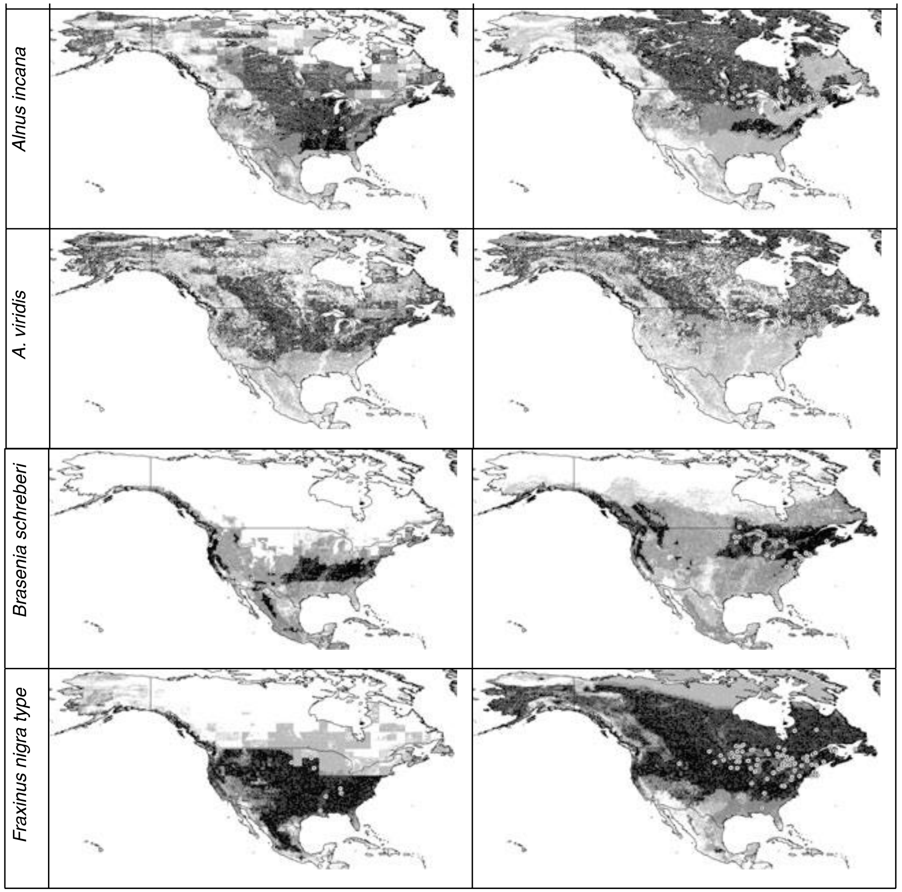

Figure 1 Summary of model predictions based on Last Glacial Maximum (LGM) occurrence data and climate information, predicting present-day occurrences. White = predicted absent by all models, light grey = predicted present by any model, dark grey = predicted present by most models (6–10), and black = predicted present by all 10 models. Known occurrence points of pollen within each period (LGM and present) are overlain; note that the LGM points are those that were used to develop models, and the present points represent the independent testing data set.

6. Creative applications

Two examples:

How Quaternary megafauna responded to climate and humans?

ARTICLE

doi:10.1038/nature10574

Species-specific responses of Late Quaternary megafauna to climate and humans

Eline D. Lorenzen[1]*, David Nogués-Bravo[2]*, Ludovic Orlando[1]*, Jaco Weinstock[1]*, Jonas Binladen[1]*, Katharine A. Marske[2]*, Andrew Ugan[3,42,43], Michael K. Borregaard[2], M. Thomas P. Gilbert[1], Rasmus Nielsen[4,5], Simon Y. W. Ho[6], Ted Goebel[7], Kelly E. Graf[7], David Byers[8], Jesper T. Stenderup[1], Morten Rasmussen[1], Paula F. Campos[1], Jennifer A. Leonard[9,10], Klaus-Peter Koepfli[11,12], Duane Froese[13], Grant Zazula[14], Thomas W. Stafford Jr[1,15], Kim Aaris-Sørensen[1], Persaram Batra[16], Alan M. Haywood[17], Joy S. Singarayer[18], Paul J. Valdes[18], Gennady Boeskorov[19], James A. Burns[20,21], Sergey P. Davydov[22], James Haile[1], Dennis L. Jenkins[23], Pavel Kosintsev[24], Tatyana Kuznetsova[25], Xulong Lai[26], Larry D. Martin[27], H. Gregory McDonald[28], Dick Mol[29], Morten Meldgaard[1], Kasper Munch[30], Elisabeth Stephan[31], Mikhail Sablin[32], Robert S. Sommer[33], Taras Sipko[34], Eric Scott[35], Marc A. Suchard[36,37], Alexei Tikhonov[32], Rane Willerslev[38], Robert K. Wayne[11], Alan Cooper[39], Michael Hofreiter[40], Andrei Sher[34]‡, Beth Shapiro[41], Carsten Rahbek[2] & Eske Willerslev[1]

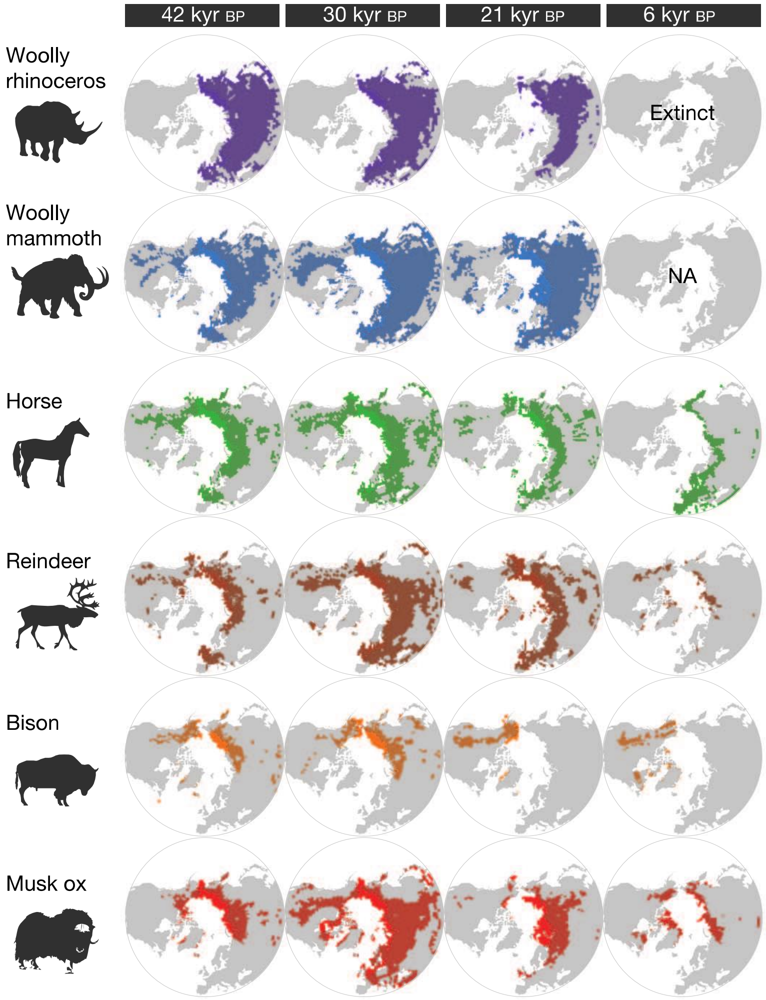

Figure 1 | Modelled potential ranges of megafauna species at 42, 30, 21 and 6 kyr BP. Ranges were modelled using the megafauna fossil record and palaeoclimatic data for temperature and precipitation; ice sheet extent was not included as a co-variable. Range measurements were restricted to the regions for which fossils were used to build the models, rather than all potentially suitable Holarctic area. NA, not available.

Can we predict the distribution of bigfoot in North America?

Journal of Biogeography (*J. Biogeogr.*) (2009)

GUEST EDITORIAL

Predicting the distribution of Sasquatch in western North America: anything goes with ecological niche modelling

J. D. Lozier[1]*, P. Aniello[2] and M. J. Hickerson[3]

¨Occurrence¨ data

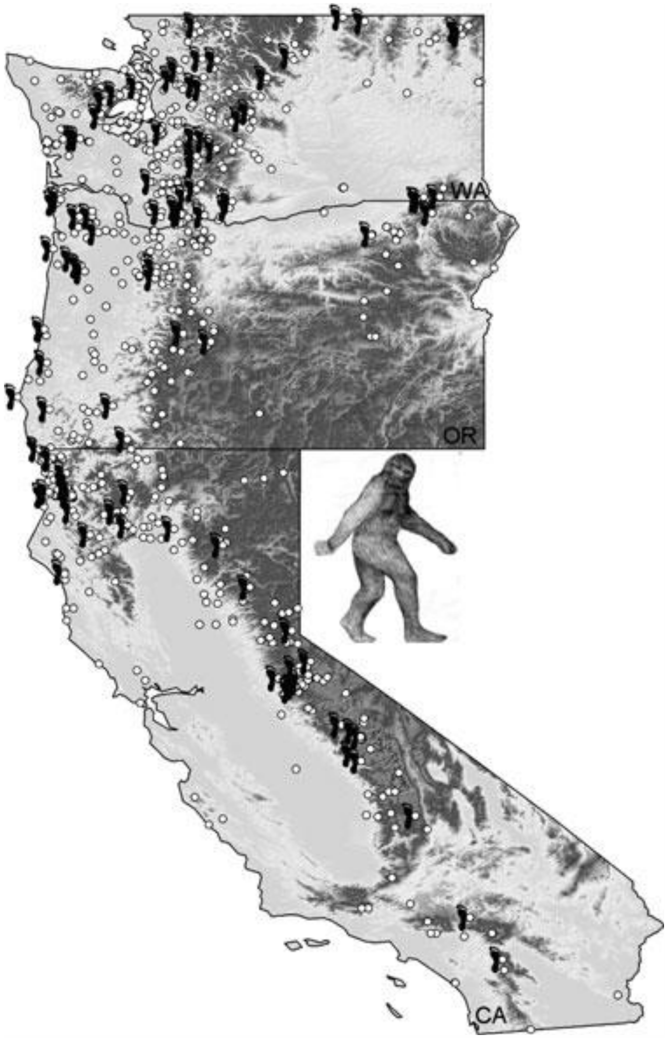

Figure 1 Map of Bigfoot encounters from Washington, Oregon and California used in the analyses. Points represent visual/auditory detection, and foot symbols represent coordinates where footprint data were available. Shading indicates topography, with lighter values representing lower elevations.

APPLICATIONS

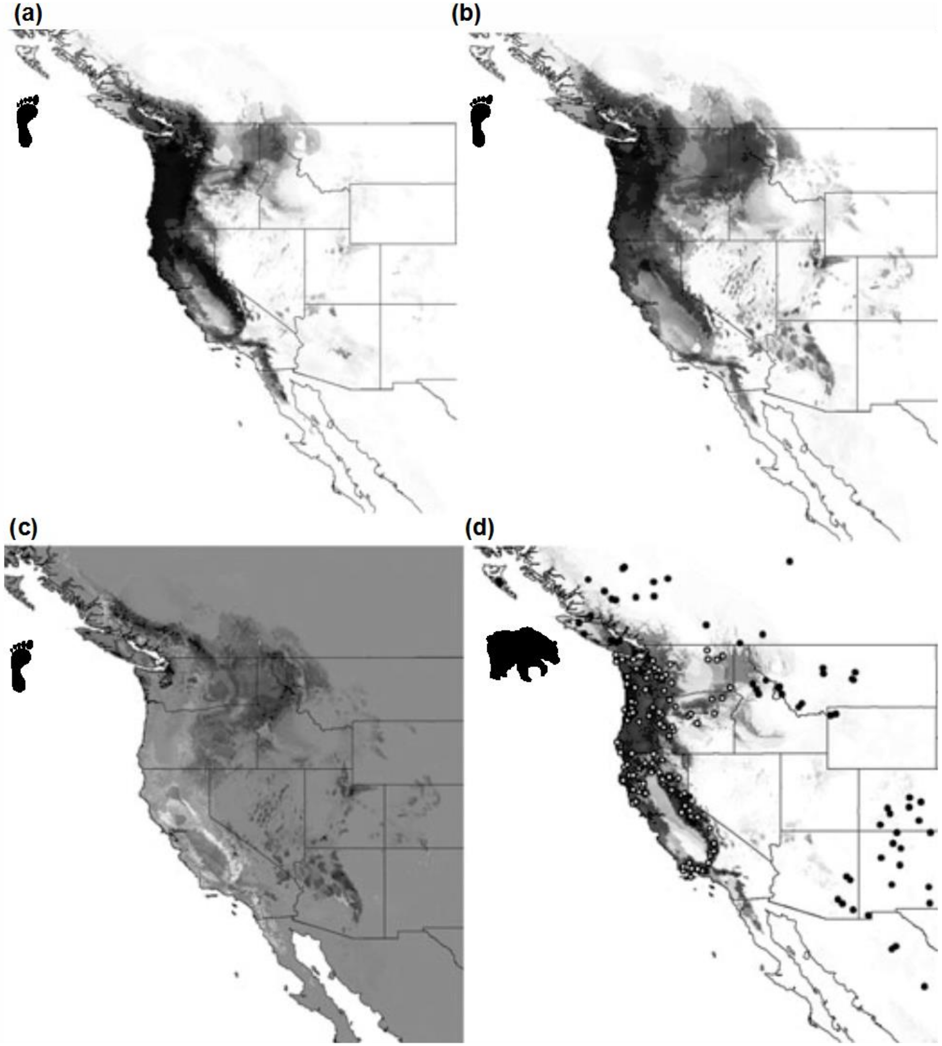

Figure 2 Predicted distributions of Bigfoot constructed from all available encounter data using maxent (a) for the present climate and (b) under a possible climate-change scenario involving a doubling of atmospheric CO_2 levels. Results are presented for logistic probabilities of occurrence ranging continuously from low (white) to high (black). Differences between (a) and (b) are shown in (c), with whiter values reflecting a decline in logistic probability of occurrence under climate change, darker values reflecting a gain, and grey reflecting no change. A predicted distribution of Ursus americanus in western North America under a present-day climate is also shown (d). White points indicate sampling localities in California, Oregon and Washington taken from GBIF (n = 113 for training, 28 for testing; compare with Fig. 1) used for the maxent model with shading as in (a) and (b); black points indicate additional known records not included in the model.